Surface Engineering of Fuel Cladding via Anodic Nanoporous Oxide for Enhanced CRUD Resistance

Jun Heo [a*], Hye Jin Jang [b], Sieun Baek [a], Sung Oh Cho [b], and Hee-Sang Shim [a]
[a] *Nuclear Materials Safety Research Division, Korea Atomic Energy Research Institute (KAERI), 989-111 Daedeok-daero, Yuseong-gu, Daejeon 305-353, Republic of Korea*
[b] *Department of Nuclear and Quantum Engineering, Korea Advanced Institute of Science and Technology, 291 Daehak-ro, Yuseong-gu, Daejeon 34141, Republic of Korea*
[*] *Corresponding author: heojun@kaeri.re.kr*

Keywords : Zirlo fuel cladding, Anodization, Nanoporous ZrO_2, Superhydrophilicity, CRUD resistance

1. Introduction

The continuous increase in reactor lifetime and power in pressurized water reactors (PWRs) demands enhanced structural integrity and operational stability of core components. Under primary coolant conditions, corrosion products generated from structural materials are transported to the core region, where subcooled nucleate boiling (SNB) occurs at the cladding-coolant interface. The interaction between boiling-induced concentration effects and transported corrosion products leads to the formation of CRUD (Chalk River Unidentified Deposits) on fuel cladding surfaces. CRUD accumulation degrades heat transfer, promotes localized corrosion, and facilitates boron hideout phenomena, potentially resulting in axial offset anomaly (AOA) and power shift events that threaten operational safety and reactor availability [1].

Various mitigation strategies have been proposed, including surface coatings and zinc injection [2,3], however, intrinsic surface modification of Zr-based cladding to regulate interfacial properties governing CRUD deposition has not been systematically explored. In this study, we propose a novel approach to develop a CRUD-resistant Zirlo cladding by forming a nanoporous zirconium oxide (ZrO_2) layer via anodic oxidation.

Anodization is a simple and environmentally benign electrochemical process capable of rapidly generating controllable oxide morphologies. The technique is scalable and applicable to large tubular geometries, making it industrially relevant for fuel cladding applications [4]. The introduction of a nanoporous oxide layer is expected to modify key surface properties, such as roughness, wettability, and zeta potential, which strongly influence particle adhesion and boiling-induced deposition behavior.

In this work, nanoporous oxide layers with controlled pore dimensions are fabricated under various anodization conditions. The resulting surface morphology and contact angle are systematically characterized to elucidate their correlation with CRUD adhesion behavior. Through this parametric study, we aim to identify surface design criteria that promote reduced particle deposition while maintaining thermal compatibility. If successfully implemented, this surface-engineered cladding concept may mitigate cladding degradation mechanisms associated with CRUD, suppress boron hideout-related power shifts, and ultimately contribute to improved operational stability and extended reactor lifetime.

2. Methods

2.1 Anodization

Zirlo sheets with a thickness of 0.48 mm were sectioned into 10 × 20 mm specimens for anodization. The samples were mechanically polished prior to processing. Before anodization, all specimens were ultrasonically cleaned in acetone and deionized (DI) water for 10 min each to remove surface contaminants. A two-electrode electrochemical system was employed for anodization, where the Zirlo specimen was used as the working electrode and a platinum sheet served as the counter electrode. The electrodes were immersed in the electrolyte with an inter-electrode distance of 30 mm. The electrolyte consisted of ethylene glycol containing 0.3 wt% NH_4F and 1 wt% DI water, which was magnetically stirred for over 3 h prior to use. Anodization was conducted at applied voltages ranging from 30 to 90 V for 5 min to investigate voltage-dependent morphological evolution. After anodization, the specimens were immediately removed from the electrolyte to minimize aging effects and subsequently ultrasonically cleaned in ethanol for 5 min to eliminate surface residues.

Post-anodization heat treatment was performed at 500 °C for 5 h in order to promote crystallization of the oxide layer and eliminate fluorine species incorporated during anodization.

2.2 Characterization

Surface morphologies of the anodized specimens were examined using scanning electron microscopy (SEM). Elemental distributions within the anodic oxide layers were analyzed via energy-dispersive spectroscopy (EDS). The crystalline phases of the heat-treated oxide layers were characterized using X-ray diffraction (XRD). As all

voltage-dependent samples exhibited similar diffraction patterns, a representative specimen was selected for phase identification.

In addition, static water contact angle measurements were conducted to evaluate the wettability of the anodized surfaces.

3. Results and Discussion

3.1 Structural Investigation

The surface morphologies of anodized Zirlo specimens fabricated under different applied voltages were compared. At the highest applied voltage (90 V), the anodized surface exhibited a relatively unstable morphology with a higher density of structural defects, as shown in Fig. 1(a). In contrast, specimens anodized at lower voltages (30 and 60 V) demonstrated comparatively more uniform and stable surface morphologies, as observed in Fig. 1(c) and (e). Magnified images in Fig. 1(b), (d), and (f) reveal the formation of nanoporous oxide layers, where the pore diameter decreases with reducing applied voltage. This trend can be attributed to the enhanced electric field strength at higher voltages, which accelerates field-assisted dissolution induced by fluorine ions, resulting in the formation of enlarged pores [5]. From a CRUD deposition perspective, pore size is expected to influence the likelihood of mechanical trapping of corrosion product particles. Excessively large pores may facilitate particle entrapment, however, image analysis indicates that the pore diameters formed under the present conditions are on the order of several tens of nanometers, which are sufficiently small to limit direct penetration of submicron corrosion product particles. Additionally, the nanoporous oxide layer surface is expected to enhance the thermal conductivity owing to its large surface area [6].

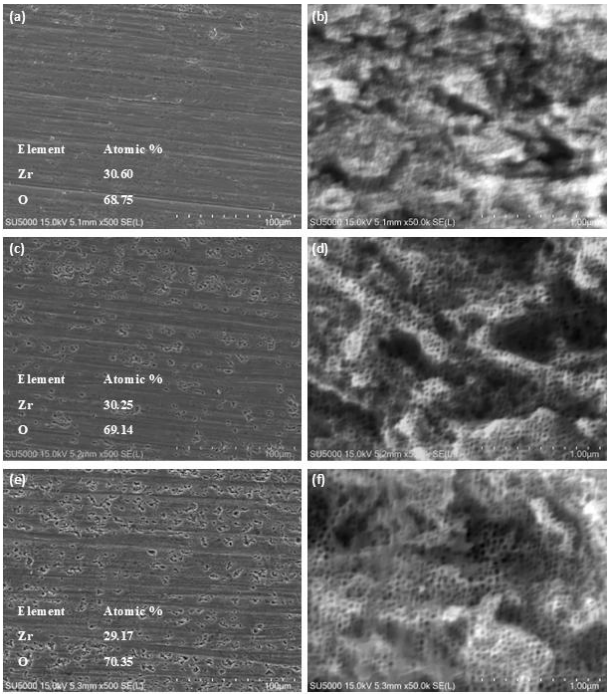

Fig. 1. SEM surface images of anodized Zirlo specimens fabricated under different applied voltages: (a,b) 30 V, (c,d) 60 V, and (e,f) 90 V. The corresponding Zr and O atomic ratios obtained from EDS analysis are indicated in (a), (c), and (e), while the magnified views of the nanoporous structures under each condition are shown in (b), (d), and (f).

EDS mapping confirmed that the anodic layers primarily consist of zirconium and oxygen. XRD analysis (Fig. 2) further revealed that the heat-treated anodized specimens exhibited distinct crystalline ZrO_2 phases, whereas the bare Zirlo sample showed only metallic zirconium peaks. These results indicate the successful formation of a nanoporous ZrO_2 layer through a relatively simple anodization process.

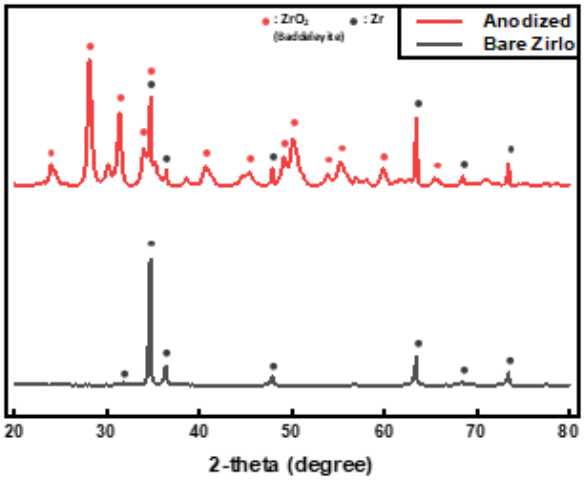

Fig. 2. X-ray diffraction (XRD) patterns of the bare Zirlo specimen and the specimen anodized at 90 V followed by heat treatment at 500 °C.

3.2 Surface Property

Static water contact angle measurements were performed to evaluate surface wettability. As shown in Fig. 3(a), the bare Zirlo specimen exhibited a contact angle of approximately 79.35°, indicating a moderately hydrophilic surface. In contrast, the anodized specimens (Fig. 3(b–d)) demonstrated significantly reduced contact angles, exhibiting superhydrophilic behavior.

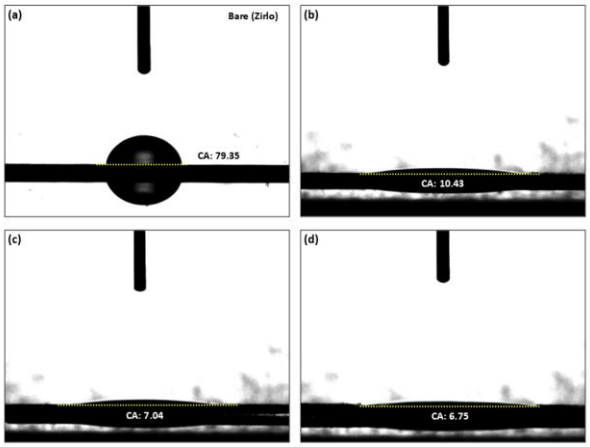

Fig. 3. Comparison of static water contact angles measured on the bare Zirlo specimen and anodized specimens: (b) 30 V, (c) 60 V, and (d) 90 V.

This enhanced wettability is likely associated with the presence of hydroxylated ZrO_2 surfaces as well as capillary-driven liquid infiltration within the nanoporous structure. In the case of specimens anodized at higher voltages (60 and 90 V), structural defects and increased surface roughness may additionally contribute to the reduction in apparent contact angle via Wenzel-type wetting behavior [7]. Considering both structural stability and potential particle trapping effects, the specimen anodized at 30 V, which exhibited relatively smaller pore diameters with uniform surface, is expected to provide a more favorable surface condition for mitigating corrosion product adhesion.

Superhydrophilic surfaces are known to promote the formation of stable hydration layers, thereby increasing the energy barrier for particle adhesion [8]. Furthermore, improved wettability may enhance liquid rewetting behavior during subcooled nucleate boiling, potentially suppressing localized dry-out and reducing the number of active nucleation sites associated with boiling-induced CRUD deposition. Further investigation, including detailed surface chemical analysis and direct CRUD deposition testing, is required to quantitatively evaluate the mitigation capability of the proposed surface modification.

4. Conclusions

In this study, nanoporous oxide layers were formed on the Zirlo cladding surfaces via anodization in order to mitigate CRUD deposition. By applying different anodization voltages (30–90 V), nanoporous ZrO_2 layers with varying surface roughness and pore sizes were successfully fabricated through a simple electrochemical process. Contact angle measurements revealed that the anodized specimens exhibited significantly lower values compared to the bare Zirlo sample, demonstrating superhydrophilic surface property.

Such enhanced wettability is expected to facilitate the formation of a stable hydration layer on the cladding surface, thereby increasing the energy barrier for corrosion product particle adhesion. In addition, improved liquid rewetting behavior may suppress localized nucleation sites associated with subcooled nucleate boiling, potentially reducing boiling-driven CRUD formation.

Based on these findings, the proposed nanoporous anodic layer is anticipated to enhance the CRUD resistance. Further investigation, including detailed surface chemical analysis and direct CRUD deposition experiments, will be conducted to quantitatively validate the mitigation capability of the engineered surface.

ACKNOWLEDGMENTS

This work was supported by the Korea Institute of Energy Technology Evaluation and Planning(KETEP) and the Ministry of Climate, Energy & Environment(MCEE) of the Republic of Korea (No. RS-2025-16065835).

REFERENCES

[1] Deshon, J., Hussey, D., Kendrick, B., McGurk, J., Secker, J., & Short, M. Pressurized water reactor fuel crud and corrosion modeling. JoM, 63(8), 64-72. 2011

[2] Li, C., Shu, R., Zhang, G., Cai, Z., Wang, J., Wang, J., ... & Liu, X. (2025). Effect of Zn injection on the CRUD deposition and corrosion behavior of a zirconium alloy under static and dynamic water conditions. Journal of Nuclear Materials, 614, 155883.

[3] Wu, Z., Xu, J., Deng, P., Zhao, Y., Yin, Z., Chen, Z., ... & Zhang, G. (2025). Crud deposition behavior on zirconium alloy and Cr coated claddings in high temperature oxygenated water: The experimental and DFT studies. Journal of Nuclear Materials, 156206.

[4] Park, Y. J., Kim, J. W., Ali, G., Kim, H. J., Addad, Y., & Cho, S. O. (2017). Fabrication of uniform nanoporous oxide layers on long cylindrical zircaloy tubes by anodization using multi-counter electrodes. Nanoscale Research Letters, 12(1), 20.

[5] Chahrour, K. M., Ahmed, N. M., Hashim, M. R., Elfadill, N. G., Maryam, W., Ahmad, M. A., & Bououdina, M. (2015). Effects of the voltage and time of anodization on modulation of the pore dimensions of AAO films for nanomaterials synthesis. Superlattices and Microstructures, 88, 489-500.

[6] Vera-Londono, L., Ruiz-Clavijo, A., Caballero-Calero, O., & Martín-González, M. (2020). Understanding the thermal conductivity variations in nanoporous anodic aluminum oxide. Nanoscale Advances, 2(10), 4591-4603.

[7] Ran, C., Ding, G., Liu, W., Deng, Y., & Hou, W. (2008). Wetting on nanoporous alumina surface: transition between Wenzel and Cassie states controlled by surface structure. Langmuir, 24(18), 9952-9955.
[8] Aspenes, G., Dieker, L. E., Aman, Z. M., Høiland, S., Sum, A. K., Koh, C. A., & Sloan, E. D. (2010). Adhesion force between cyclopentane hydrates and solid surface materials. Journal of colloid and interface science, 343(2), 529-536.